Supporting Information

Low-Power Photon Upconversion in Organic Glasses

Roberto Vadrucci, Christoph Weder, and Yoan C. Simon**

Adolphe Merkle Institute, University of Fribourg, Rte de l'Ancienne Papeterie,
CH-1723 Marly 1, Switzerland

R. Vadrucci, Dr. Y. C. Simon, Prof. Dr. C. Weder
Adolphe Merkle Institute, University of Fribourg
Rte de l'Ancienne Papeterie, CH-1723 Marly 1, Switzerland
[*] e-mail: yoan.simon@unifr.ch christoph.weder@unifr.ch
Homepage: http://www.am-institute.ch/en

Table of Contents

1. Materials and Methods

PdOEP [2,3,7,8,12,13,17,18-octaethyl-21H,23H-porphine palladium(II), dye content 85%], PtOEP [2,3,7,8,12,13,17,18-octaethyl-21H,23H-porphine platinum(II), dye content 98%], 4-(hydroxymethyl)phenylboronic acid, tetrakis(triphenylphosphine)palladium(0) [$Pd(PPh_3)_4$], barium hydroxide monohydrate, and N,N-dimethylformamide (DMF, ACS grade) were purchased from Sigma-Aldrich and were used as received. 9,10-diphenylanthracene (DPA, 97%) was purchased from Sigma-Aldrich and purified by sublimation under vacuum (ca. 10^{-2} mbar). Spectroscopic grade toluene was purchased from Acros Organics. Dichloromethane for optical film preparation (DCM, ACS HPLC grade with alcoholic or olefinic stabilizer) was purchased from Honeywell. 9-Bromo-10-phenyl anthracene was synthesized according to the method reported by Zhang *et al*.[1]

Microwave-assisted syntheses were performed with a Biotage®Initiator Microwave Synthesizer and column chromatography was performed with a Biotage®IsoleraOne. Optical fluorescence microscopy images were acquired on an Olympus BX51 microscope. Samples were irradiated at a wavelength of 330-385 nm and emission detected at wavelengths of >420 nm. UV-Vis absorption spectra were recorded on an Shimadzu UV-2401PC.

NMR spectroscopic data were measured on a Bruker Avance DPX (^{1}H NMR: 360 MHz, ^{13}C NMR: 90.5 MHz) and on a Bruker Avance III spectrometer (^{1}H NMR: 300 MHz, ^{13}C NMR: 75.5 MHz). Elemental analyses were provided by the School of Engineering EIF-ISF Fribourg, Switzerland and mass spectra were acquired by the Analytical Services of the Chemistry Department at the University of Fribourg, Switzerland.

2. Syntheses

Synthesis of 9-(4-hydroxymethylphenyl)-10-phenyl anthracene (DPA-CH_2OH)

A 20 mL microwave vessel was charged with 9-bromo-10-phenylanthracene (1.5 g, 4.5 mmol), (4-hydroxymethyl) phenylboronic acid (752 mg, 4.95 mmol, 1.1 eq.) and $Ba(OH)_2 \cdot H_2O$ (2.57 g, 13.5 mmol, 3 eq.). DMF (20 mL) and water (1 mL) were added to form a yellow mixture. $Pd(PPh_3)_4$ (31.2 mg, 27 μmol, 0.6 mol%) was quickly added to the mixture before sealing the vessel. The reaction mixture was purged with argon for 15 min, subsequently stirred for 5 min at RT and finally heated to 150°C for 15 min at 3-4 bar in the microwave synthesizer. A yellowish solution over a brownish-greyish precipitate was obtained.

The reaction mixture was filtered, the filtrate collected and the solid residue was extracted with toluene (100 mL). The extracted solution was filtered through a pad of celite, which was washed with an additional amount of toluene (30 mL). The filtrates were collected and the solvents removed under reduced pressure. Residual DMF was removed by extracting the solid obtained with water (2x10 mL). The powder was re-dissolved in DCM (60 mL), the solution then washed with 0.1M NaOH (3x100 mL), water (3x100 mL), brine (3x50 mL) and dried over anhydrous $MgSO_4$. The organic fraction was collected and solvent was removed *in vacuo*. The residue re-dissolved in warm toluene (40 mL) and the solution concentrated to a volume of ~5 mL. Addition of hexanes (40 mL) led to precipitation of a fine, off-white solid. The off-white solid was sublimed at 215°C under vacuum (ca. 10^{-2} mbar) for 16 h. 890 mg (55 %) of bright yellow crystals were obtained.

T_m = 218°C (Fig. 2a, 1st heating cycle, heating rate 10°C/min)

Elemental Analysis: Found: C, 89.9; H, 5.65. Calc. for $C_{27}H_{20}O$: C, 89.97; H, 5.59%

^{1}H NMR (360 MHz, $CDCl_3$): δ (ppm) = 7.82-7.67 (m, 4H, CH^{Ar}), 7.66-7.43 (m, 9H, CH^{Ar}), 7.42-7.28 (m, 4H, CH^{Ar}), 4.91 (s, 2H, $C\underline{H_2}OH$), 1.88 (s, 1H, $CH_2O\underline{H}$).

^{13}C APT NMR (90.5 MHz, $CDCl_3$): δ (ppm) = 140.2 (s, C^{Ar}), 139.2 (s, C^{Ar}), 138.7 (s, C^{Ar}), 137.3 (s, C^{Ar}), 136.9 (s, C^{Ar}), 131.7 (s, CH^{Ar}), 131.5 (s, CH^{Ar}), 130.0 (s, C^{Ar}), 128.6 (s, CH^{Ar}), 127.6 (s, CH^{Ar}), 127.3 (s, CH^{Ar}), 127.2 (s, CH^{Ar}), 127.0 (s, CH^{Ar}), 125.2 (s, CH^{Ar}), 65.5 (s, CH_2).

MS (MALDI): *m/z* 360.15 (M^+)

Synthesis of 9,10-bis(4-hydroxymethylphenyl) anthracene (DPA-$(CH_2OH)_2$)

A 20 mL microwave vessel was charged with 9,10-dibromo anthracene (500 mg, 1.5 mmol), 4-(hydroxymethyl) phenylboronic acid (475 mg, 3.12 mmol, 2.1 eq.) and $Ba(OH)_2 \cdot H_2O$ (845 mg, 4.5 mmol, 3 eq.). DMF (15 mL) and water (5 mL) were added to form a yellow mixture. $Pd(PPh_3)_4$ (34.4 mg, 29.5 µmol, 2 mol%) was quickly added to the mixture before sealing the vessel. The reaction mixture was purged with argon for 15 min, subsequently stirred for 5 min at RT and finally heated to 150°C for 15 min at 3-4 bar in the microwave synthesizer. A yellowish solution over a grey precipitate was obtained.

The reaction mixture was filtered, the filtrate collected and the solid grey residue extracted with ethyl acetate (60 mL) and ethyl acetate/EtOH (60 mL, 1:1). The combined extracts were filtered through a pad of celite, collected and the solvents removed under reduced pressure to give a white solid. The solid residue was then purified by column chromatography on silicagel (toluene : ethyl acetate 2:1, $R_f = 0.24$) to obtain 140 mg (24%) of a yellowish powder.

$T_m > 300°C$ (Fig. S10, 1st heating cycle, heating rate 10°C/min)

^1H NMR (300 MHz, DMSO-d_6): δ (ppm) = 7.63-7.57 (m, 8H, CH^{Ar}), 7.44-7.38 (m, 8H, CH^{Ar}), 5.35 (t, J = 5.8 Hz, 2H, $CH_2O\underline{H}$), 4.70 (d, J = 5.8 Hz, 4H, $C\underline{H}_2OH$).

^{13}C APT NMR (75.5 MHz, DMSO-d_6): δ (ppm) = 142.1 (s, C^{Ar}), 136.6 (s, C^{Ar}), 136.4 (s, C^{Ar}), 130.7 (s, CH^{Ar}), 129.3 (s, C^{Ar}), 126.7 (s, CH^{Ar}), 126.5 (s, CH^{Ar}), 125.4 (s, CH^{Ar}), 62.5 (s, CH_2).

MS (MALDI): *m/z* 390.16 (M^+)

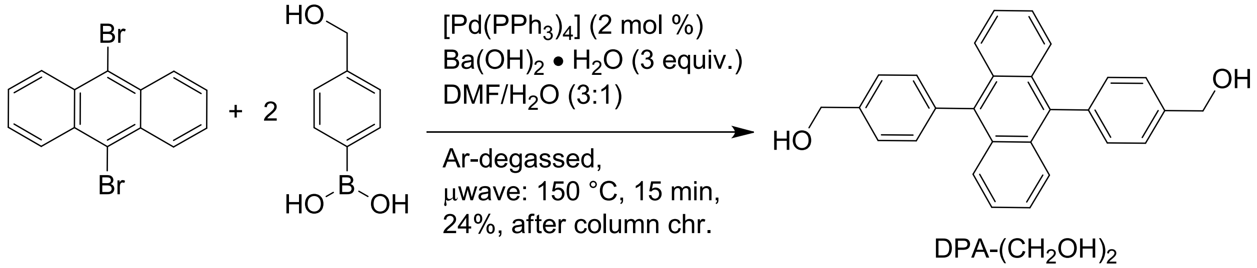

Scheme S1. Microwave-assisted Suzuki-Miyaura synthesis of 9,10-bis(4-hydroxymethylphenyl) anthracene (DPA-$(CH_2OH)_2$).

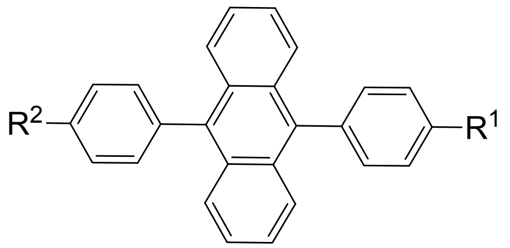

Substance	Residue	T_m / °C
DPA	$R_1 = R_2 = H$	251
DPA-CH_2OH	$R_1 = CH_2OH$, $R_2 = H$	218
DPA-$(CH_2OH)_2$	$R_1 = R_2 = CH_2OH$	>300

Fig. S1. Melting temperatures, T_m (1st heating cycle, heating rate 10°C/min), of DPA and DPA derivatives.

3. NMR-Spectra

9-(4-Hydroxymethylphenyl)-10-phenyl anthracene (DPA-CH$_2$OH)

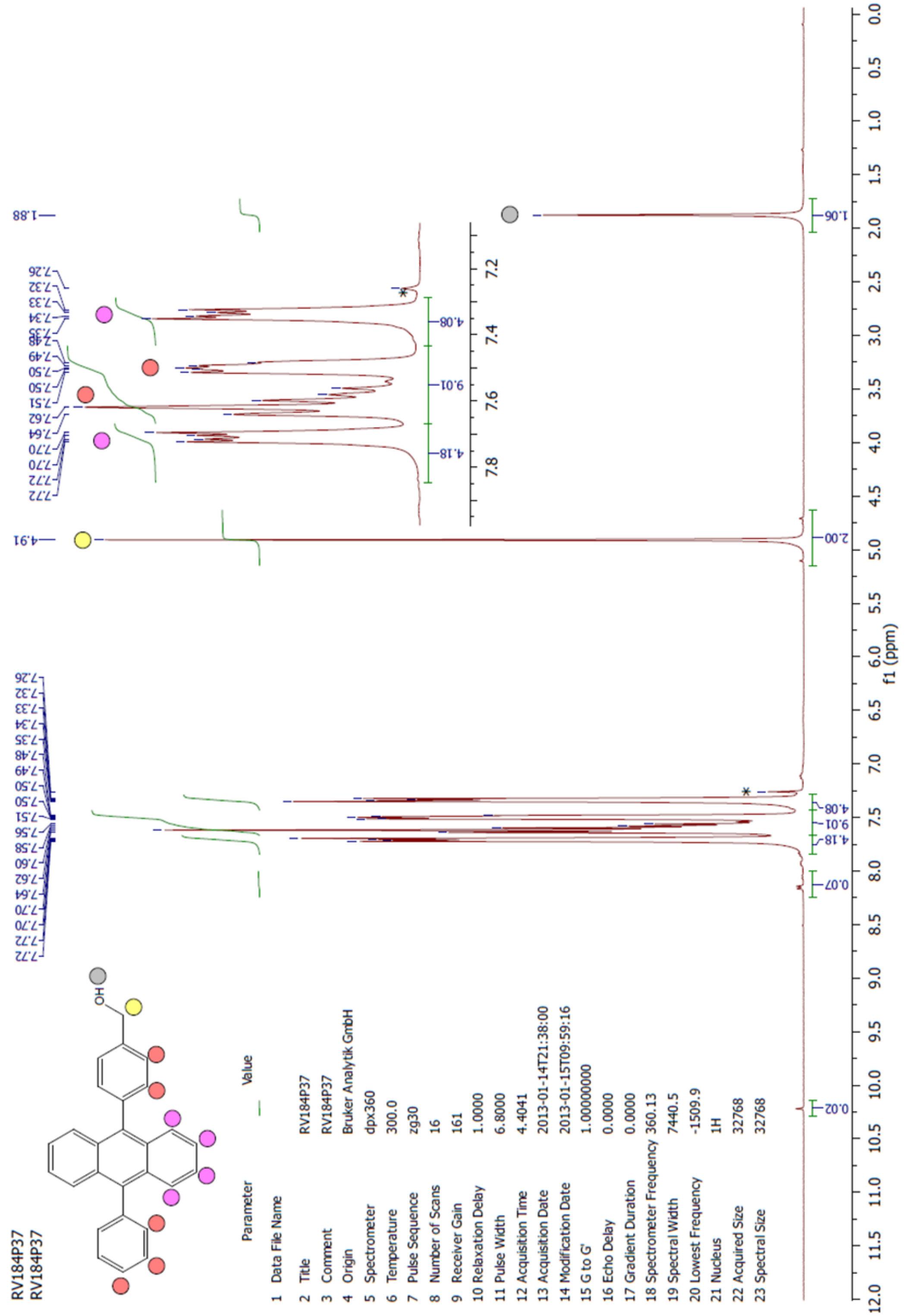

	Parameter	Value
1	Data File Name	
2	Title	RV184P37
3	Comment	RV184P37
4	Origin	Bruker Analytik GmbH
5	Spectrometer	dpx360
6	Temperature	300.0
7	Pulse Sequence	zg30
8	Number of Scans	16
9	Receiver Gain	161
10	Relaxation Delay	1.0000
11	Pulse Width	6.8000
12	Acquisition Time	4.4041
13	Acquisition Date	2013-01-14T21:38:00
14	Modification Date	2013-01-15T09:59:16
15	G to G'	1.00000000
16	Echo Delay	0.0000
17	Gradient Duration	0.0000
18	Spectrometer Frequency	360.13
19	Spectral Width	7440.5
20	Lowest Frequency	-1509.9
21	Nucleus	1H
22	Acquired Size	32768
23	Spectral Size	32768

Figure S2. ^{1}H NMR spectrum of 9-(4-hydroxymethylphenyl)-10-phenyl anthracene in CDCl$_3$.

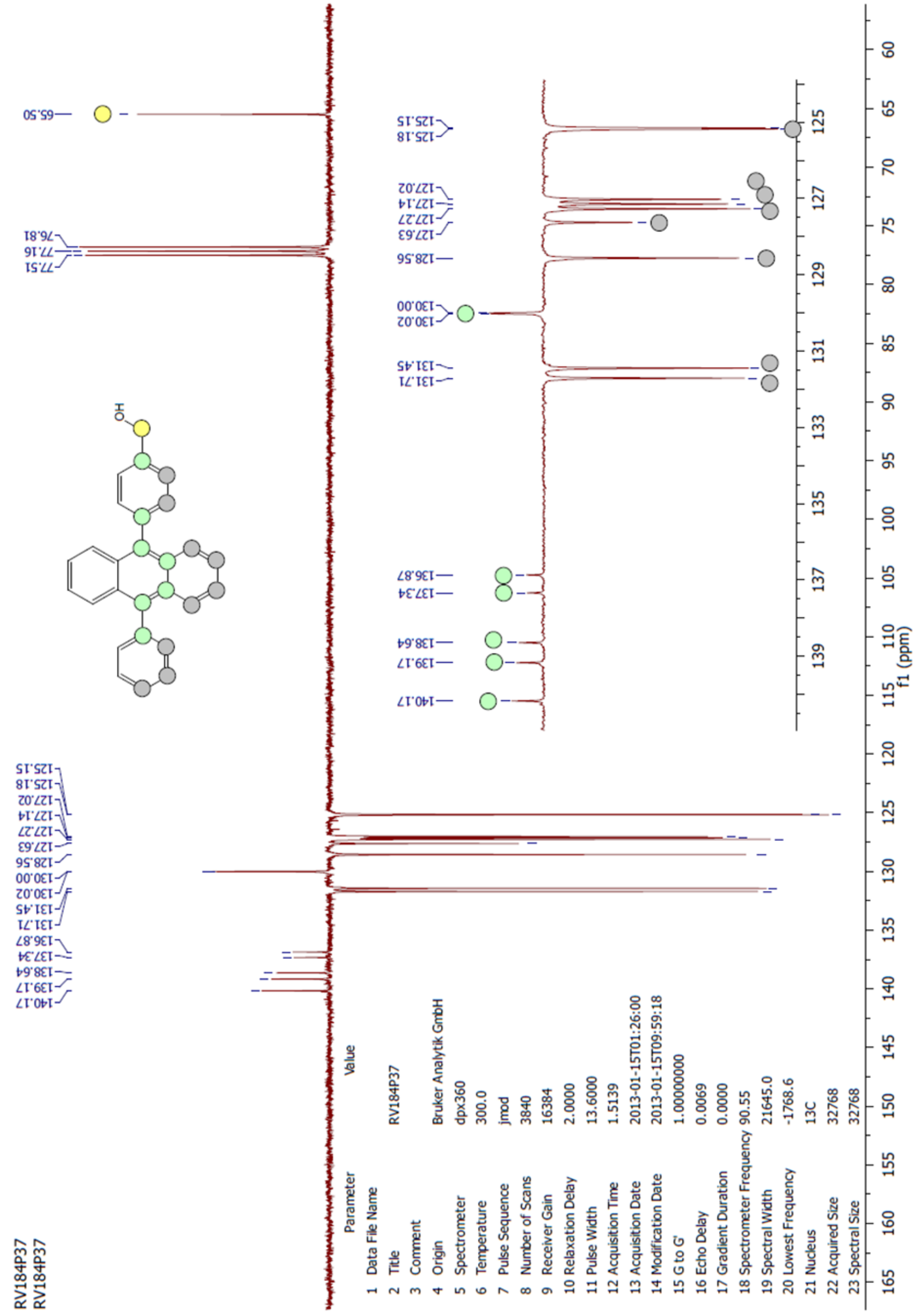

Parameter	Value
1 Data File Name	
2 Title	RV184P37
3 Comment	
4 Origin	Bruker Analytik GmbH
5 Spectrometer	dpx360
6 Temperature	300.0
7 Pulse Sequence	jmod
8 Number of Scans	3840
9 Receiver Gain	16384
10 Relaxation Delay	2.0000
11 Pulse Width	13.6000
12 Acquisition Time	1.5139
13 Acquisition Date	2013-01-15T01:26:00
14 Modification Date	2013-01-15T09:59:18
15 G to G'	1.00000000
16 Echo Delay	0.0069
17 Gradient Duration	0.0000
18 Spectrometer Frequency	90.55
19 Spectral Width	21645.0
20 Lowest Frequency	-1768.6
21 Nucleus	13C
22 Acquired Size	32768
23 Spectral Size	32768

Figure S3. ^{13}C APT NMR spectrum of 9-(4-hydroxymethylphenyl)-10-phenyl anthracene in $CDCl_3$.

9,10-Di(4-hydroxymethylphenyl) anthracene (DPA-(CH_2OH)$_2$)

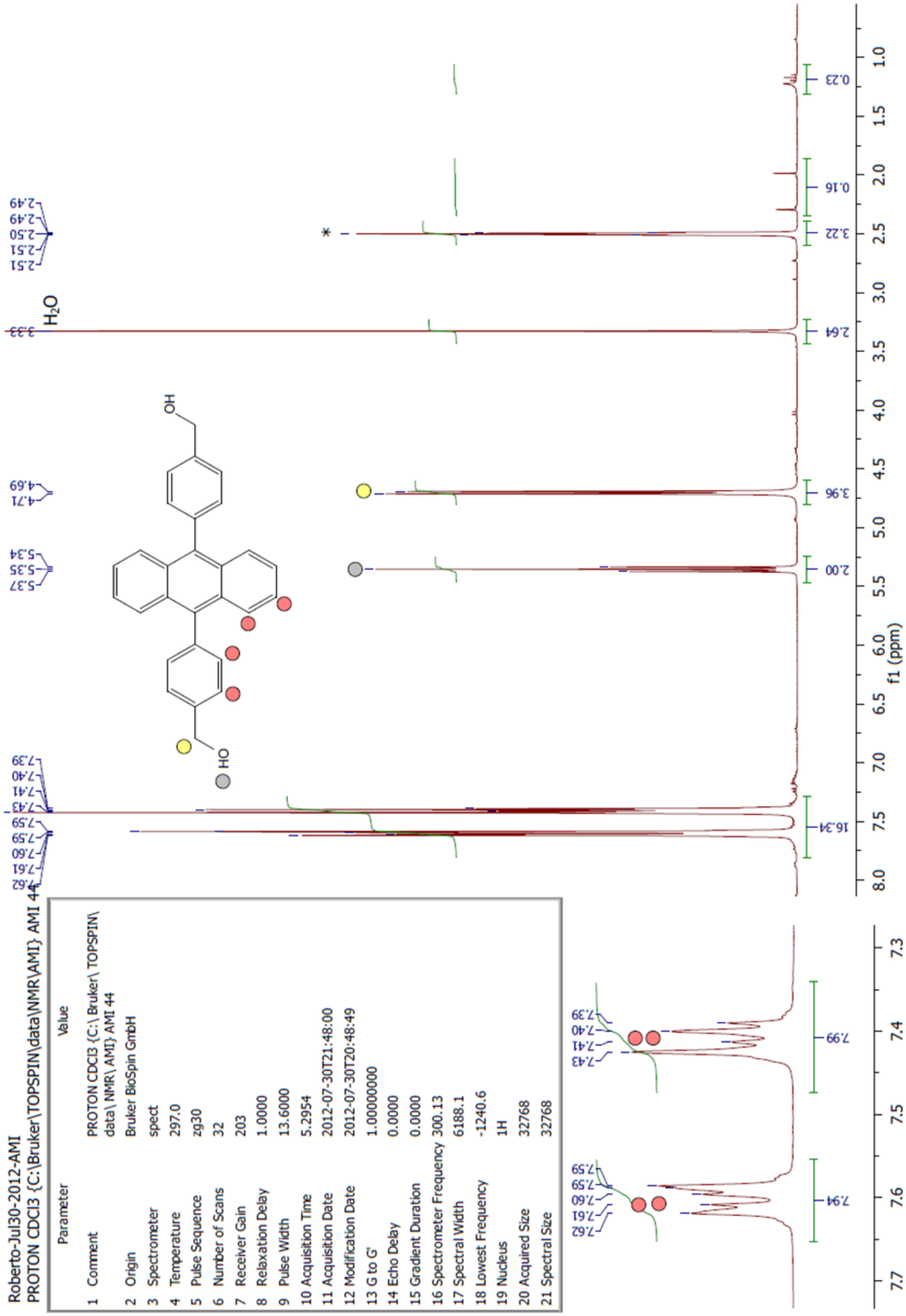

Roberto-Jul30-2012-AMI
PROTON CDCl3 {C:\Bruker\TOPSPIN\data\NMR\AMI} AMI 44

	Parameter	Value
1	Comment	PROTON CDCl3 {C:\ Bruker\ TOPSPIN\ data\ NMR\ AMI} AMI 44
2	Origin	Bruker BioSpin GmbH
3	Spectrometer	spect
4	Temperature	297.0
5	Pulse Sequence	zg30
6	Number of Scans	32
7	Receiver Gain	203
8	Relaxation Delay	1.0000
9	Pulse Width	13.6000
10	Acquisition Time	5.2954
11	Acquisition Date	2012-07-30T21:48:00
12	Modification Date	2012-07-30T20:48:49
13	G to G'	1.00000000
14	Echo Delay	0.0000
15	Gradient Duration	0.0000
16	Spectrometer Frequency	300.13
17	Spectral Width	6188.1
18	Lowest Frequency	-1240.6
19	Nucleus	1H
20	Acquired Size	32768
21	Spectral Size	32768

Figure S4. ^{1}H NMR spectrum of 9,10-di(4-hydroxymethylphenyl) anthracene in DMSO-d_6.

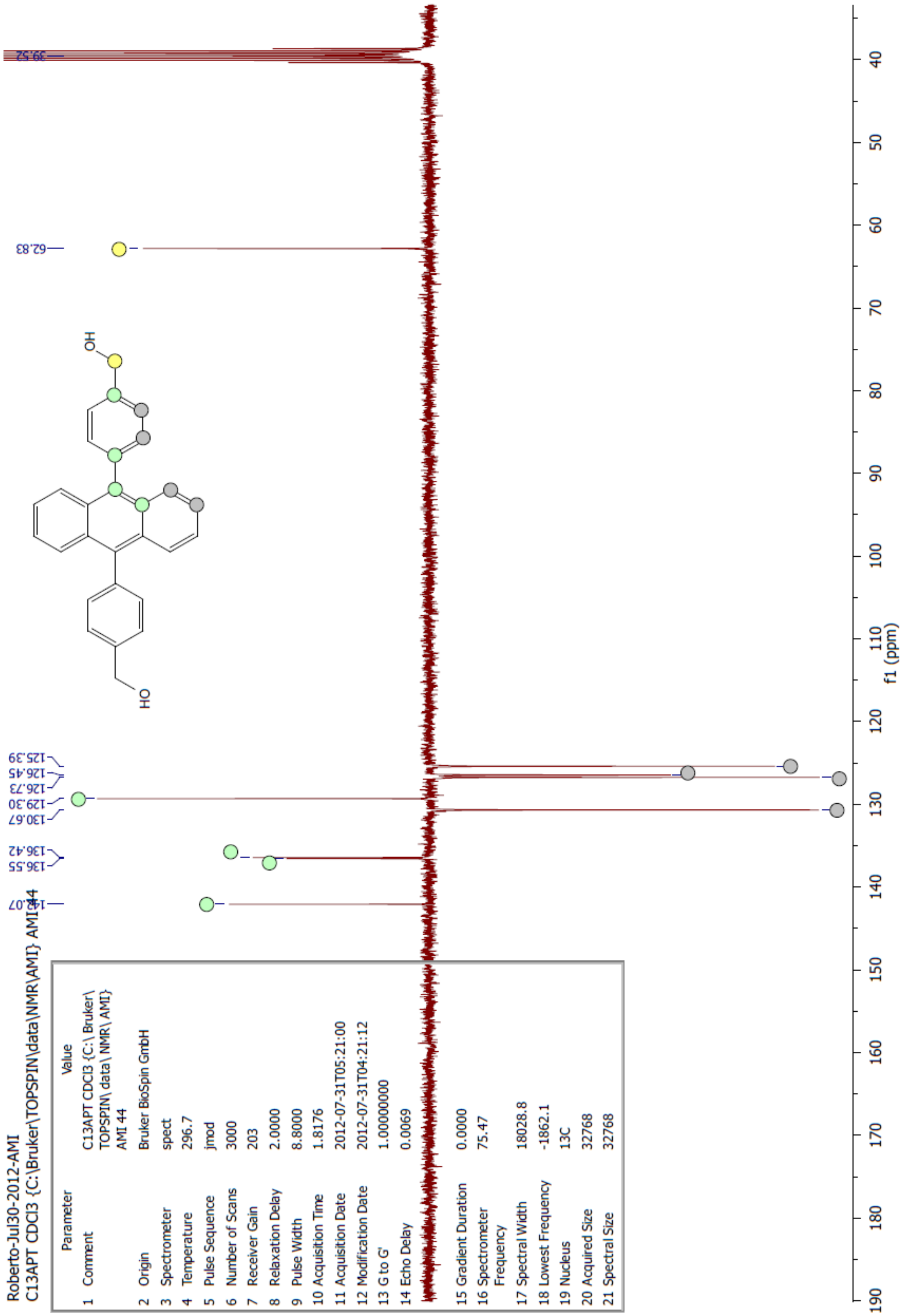

	Parameter	Value
1	Comment	C13APT CDCl3 {C:\Bruker\TOPSPIN\data\NMR\AMI} AMI 44
2	Origin	Bruker BioSpin GmbH
3	Spectrometer	spect
4	Temperature	296.7
5	Pulse Sequence	jmod
6	Number of Scans	3000
7	Receiver Gain	203
8	Relaxation Delay	2.0000
9	Pulse Width	8.8000
10	Acquisition Time	1.8176
11	Acquisition Date	2012-07-31T05:21:00
12	Modification Date	2012-07-31T04:21:12
13	G to G'	1.00000000
14	Echo Delay	0.0069
15	Gradient Duration	0.0000
16	Spectrometer Frequency	75.47
17	Spectral Width	18028.8
18	Lowest Frequency	-1862.1
19	Nucleus	13C
20	Acquired Size	32768
21	Spectral Size	32768

Figure S5. ^{13}C APT NMR spectrum of 9,10-di(4-hydroxymethylphenyl) anthracene in DMSO-d_6.

4. MALDI-Mass Spectra

9-(4-Hydroxymethylphenyl)-10-phenyl anthracene (DPA-CH_2OH)

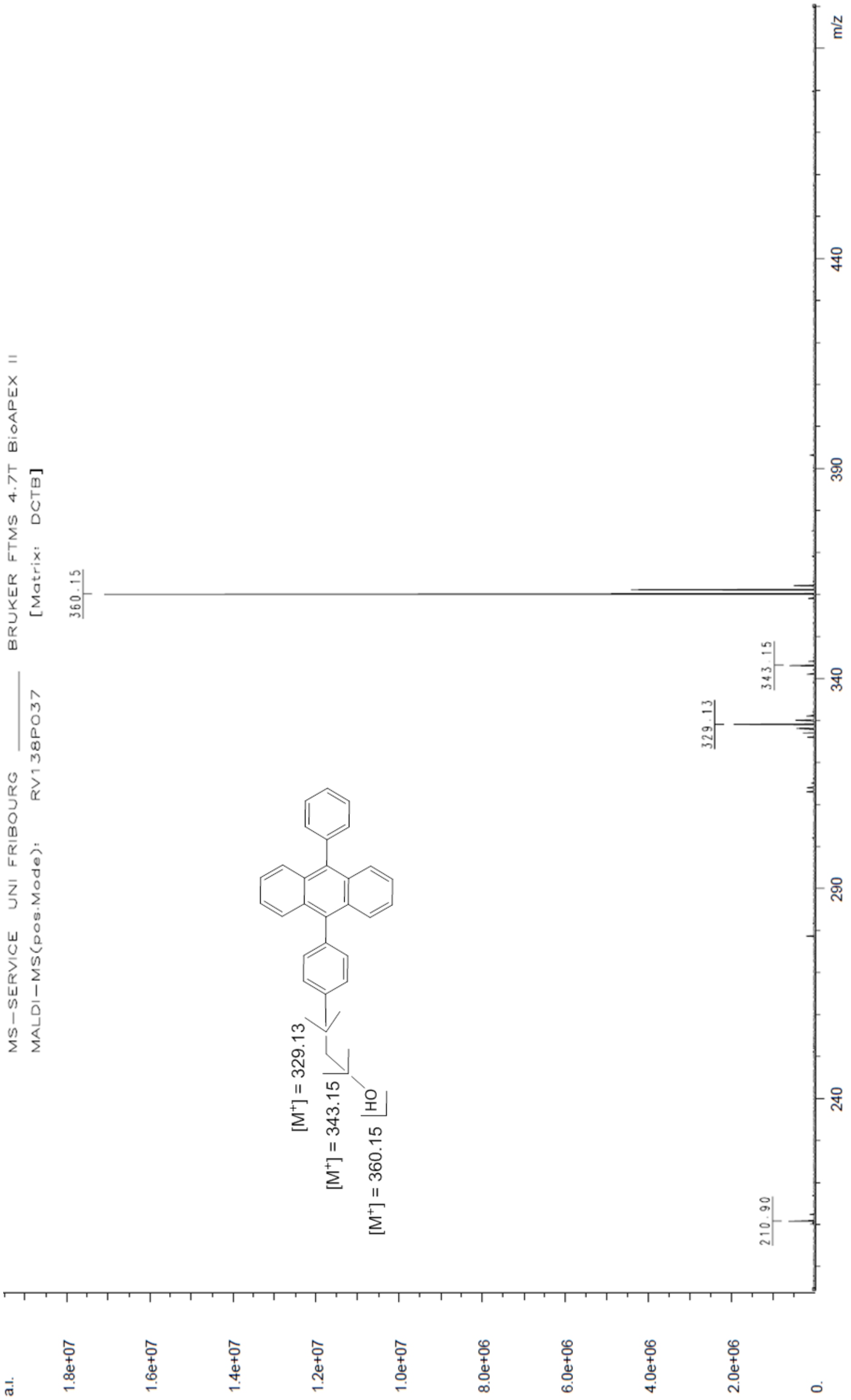

Figure S6. MALDI spectrum of 9-(4-hydroxymethylphenyl)-10 phenyl anthracene.

9,10-Di(4-hydroxymethylphenyl) anthracene (DPA-(CH_2OH)$_2$)

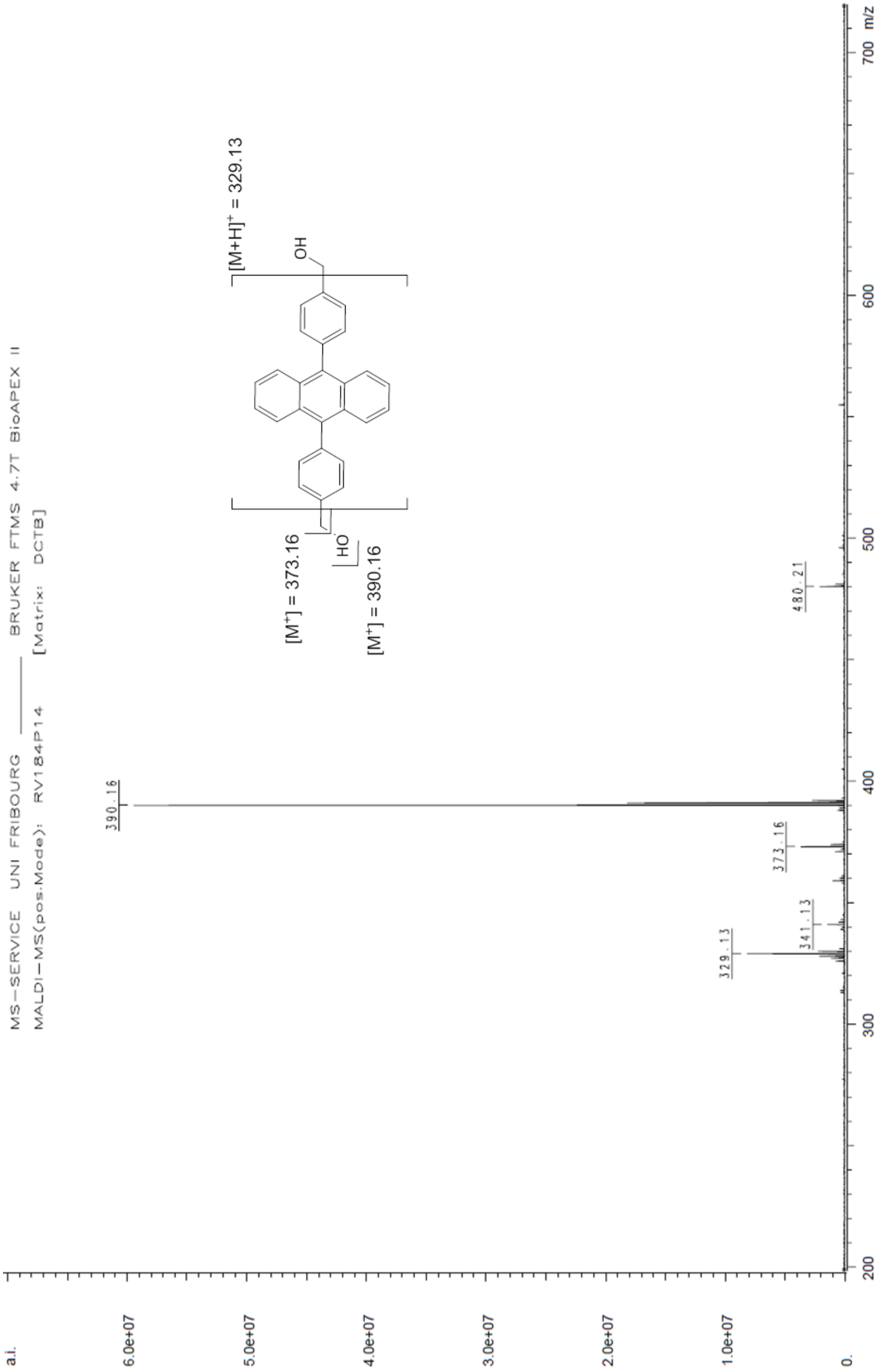

Figure S7. MALDI spectrum of 9,10-di(4-hydroxymethylphenyl) anthracene.

5. DSC and TGA

Differential scanning calorimetry (DSC) measurements were performed using a Mettler-Toledo DSC-1 equipped with a Huber TC100 cooling regulation system. Thermal gravimetric analysis (TGA) measurements were performed on a Mettler Toledo TGA/DSC thermogravimetric analyzer. DSC and TGA measurements were performed under nitrogen.

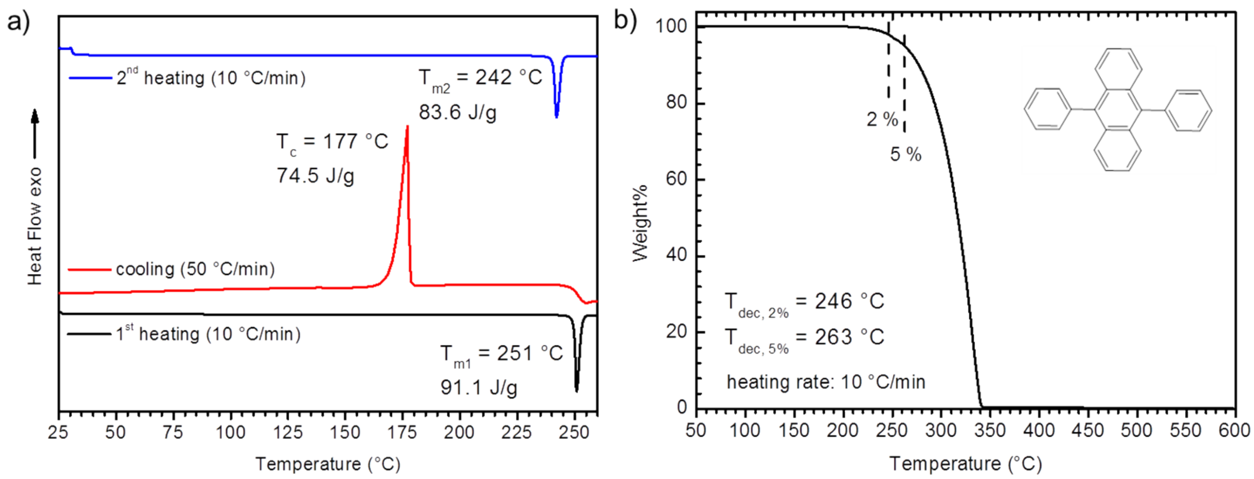

Figure S8. a) DSC traces (first heating, cooling, second heating) and b) TGA traces of vacuum-sublimed 9,10-diphenylanthracene (DPA). Heating and cooling rates, as well as the enthalpies of the various transitions are indicated in the graphs.

The melting point of DPA after the 2nd heating cycle T_{m2} = 242°C is reduced by 9°C with respect to the value determined in the first heating cycle T_{m1} = 251°C. This difference may reflect crystallization into a different polymorph during fast cooling or mild decomposition into products that depress the melting point.

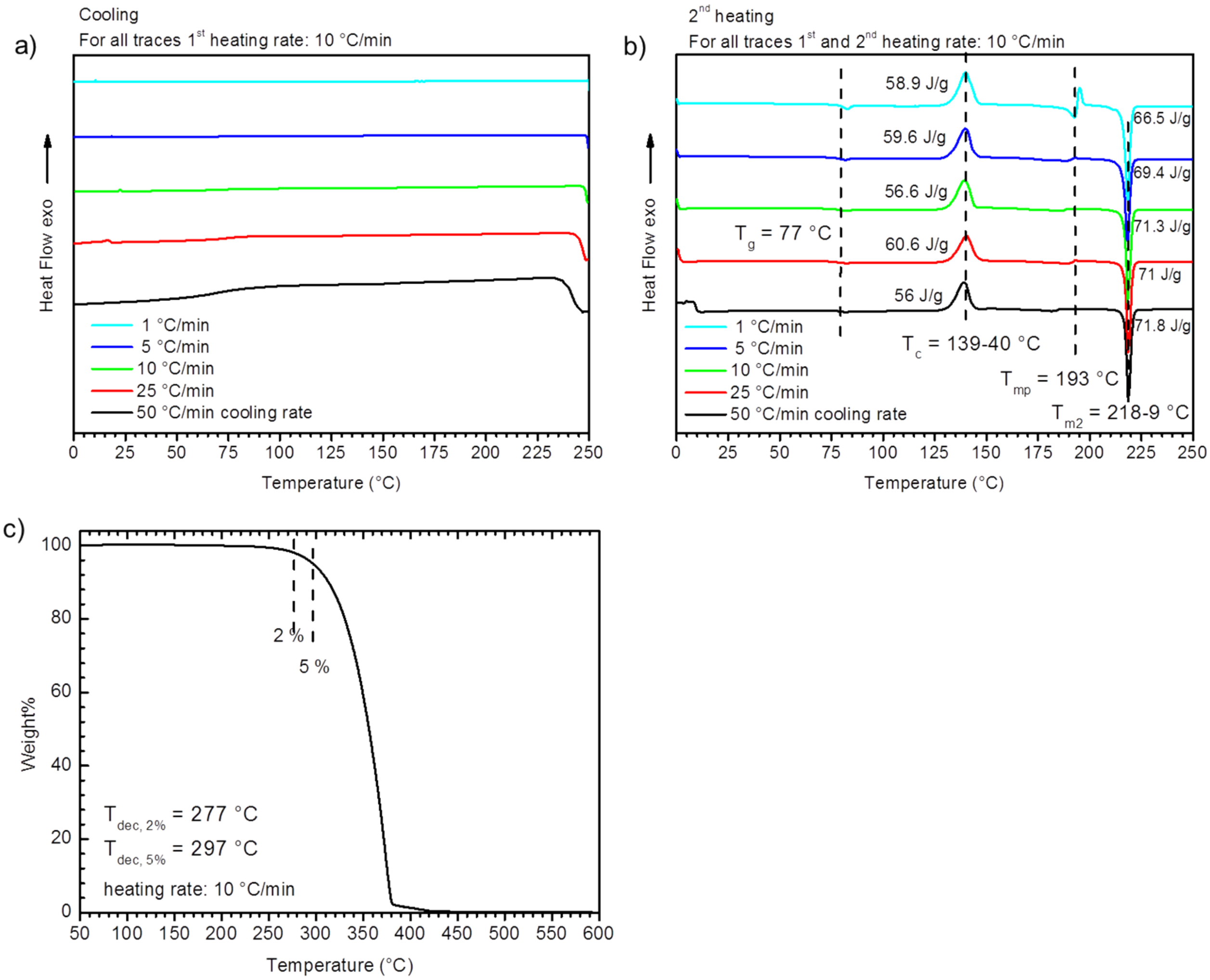

Fig. S9. a), b) DSC (cooling and second heating of samples cooled at different rates) and c) TGA traces of as-prepared 9-(4-hydroxymethylphenyl)-10-phenyl anthracene (DPA-CH_2OH). Heating and cooling rates, as well as the enthalpies of the various transitions are indicated in the graphs.

DSC traces of DPA-CH_2OH with higher cooling rates (5 to 50°C/min) are virtually identical to the ones shown here for a cooling rate of 1°C/min except for a minor polymorph melting at 193°C appearing in the latter. TGA shows a higher thermal stability for DPA-CH_2OH than for DPA (Fig. S8).

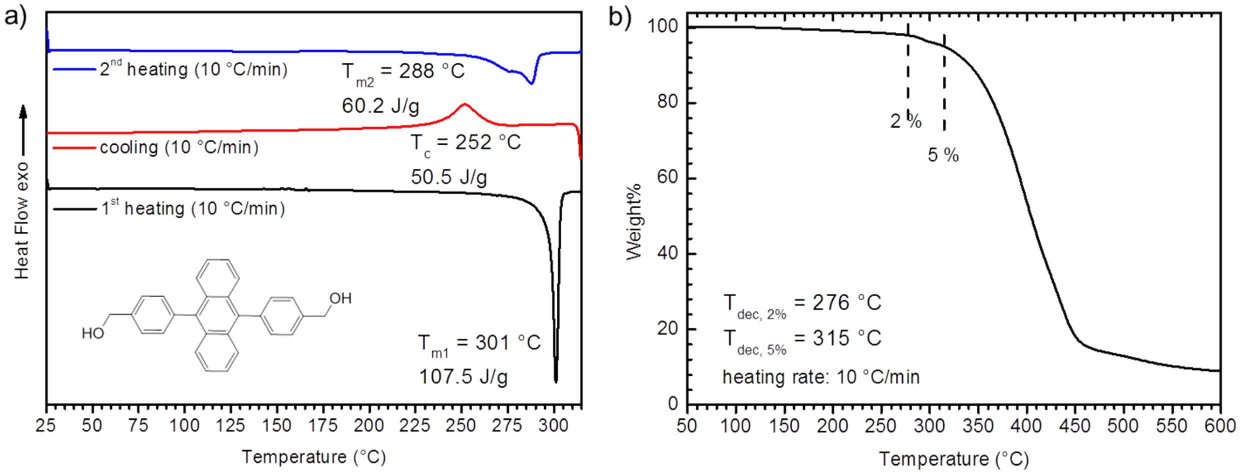

Fig. S10. a) DSC (first heating, cooling, second heating) and b) TGA traces of 9,10-di(4-hydroxymethylphenyl) anthracene (DPA-(CH_2OH)$_2$). Heating and cooling rates, as well as the enthalpies of the various transitions are indicated in the graphs.

In the 2nd heating cycle, DPA-(CH_2OH)$_2$ displayed a broad T_{m2}, reduced by 13°C compared to T_{m1}. This may be explained by crystallization into a different polymorph upon cooling of the melt at a rate of 10°C/min. Decomposition setting in at $T < T_m$ (TGA) may create impurities being responsible for the broad peak T_{m2}. In contrast to DPA-CH_2OH, no molecular glass formation can be observed at the given cooling rate.

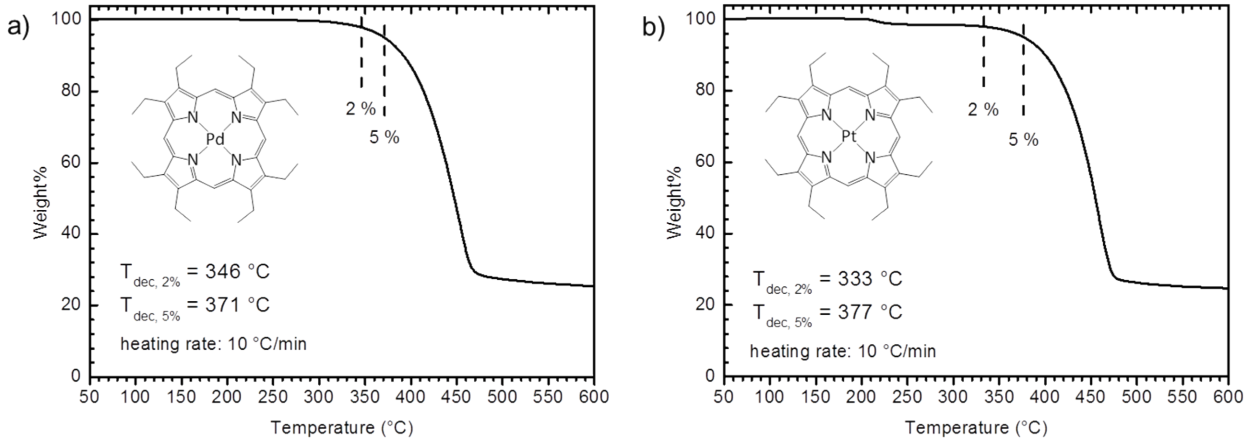

Fig. S11. TGA traces of a) PdOEP and b) PtOEP.

Table S1. Decomposition onset temperatures $T_{dec, 2\%}$ (2% onset) of DPA-CH_2OH, PdOEP and PtOEP. For all substances $T_{dec, 2\%} > T_m$ (DPA-CH_2OH).

Substance	T_m / °C	$T_{dec, 2\%}$ / °C
DPA-CH_2OH	218	277
PdOEP		346
PtOEP		333

6. Powder X-Ray Diffraction (PXRD) Experiments

PXRD measurements were performed on a Philips PW 1800 diffractometer using a Cu Kα radiation. Samples were first dispersed in water and subsequently dried on a silicon substrate. The XRD data were analyzed by Rietveld method using Topas 3 (Bruker Inc.) program.

Amorphous DPA-CH_2OH was produced between glass slides using the same procedure as for the production of the upconverting molecular glasses (see Section 7). The PXRD sample was obtained by removing the MG from the glass slide and pulverizing it.

7. Preparation of Molecular Glass Films

Pre-mixing of Sensitizer and Emitter

DPA-CH_2OH (32 mg) was dissolved in a dichloromethane solution (4-5 mL) containing the appropriate amount of PdOEP or PtOEP, resulting in clear, rose or red solutions respectively. Solvent and solution transfers were performed with glass syringes under ambient conditions. The solvent was quickly evaporated *in vacuo* at 500 mbar and 50°C in order to obtain rose or red powders respectively.

Preparation of Molecular Glass Films

Two methods were utilized for the preparation of upconverting molecular glasses. In Method A, heating and cooling rates were well controlled in order to permit independent reproduction of the data. In Method B, which was designed as a higher-throughput process to prepare many samples quickly, the melts were cooled as quickly as possible by using a room temperature nitrogen flow, but the cooling rate is not exactly known. Method A (high cooling rate of 40 °C/min) and B afforded samples that display similar UC efficiencies, which shows that they can be used interchangeably.

Method A: Samples were prepared by sandwiching premixed sensitizer/emitter powder, or the neat emitter (ca. 15 mg), between two microscopy slides (1 mm thick, Marienfeld) that were separated by two 90 µm thick aluminum sheets. Samples were placed into a Linkam LTS350 heating and freezing microscope stage and put under constant nitrogen flow. Subsequently, samples were heated from 25°C to 150°C with a heating rate of 40°C/min, to 250°C with a heating rate of 10°C/min and immediately cooled to 25°C with cooling rates ranging from 40 to 10°C/min.

Method B: The premixed sensitizer/emitter powder, or alternatively of the neat emitter (ca. 15 mg), was sandwiched between two microscopy slides (1 mm thick, Marienfeld) that were separated by two 90 µm thick aluminum sheets. This sandwich was introduced into a 100 mL Erlenmeyer flask, which was evacuated under vacuum (ca. 10^{-2} mbar) for 15 min and then backfilled with nitrogen. Three such cycles were applied. The bottom of the flask, which was in close contact with the sample, was heated with a heatgun until the powder had turned into a clear melt (2000 W, 80 sec). The sample was subsequently cooled by using a RT nitrogen flow. The glass slide sandwich containing a red, transparent film was subsequently removed from the Erlenmeyer flask and the borders were sealed with hot glue. Often, some minutes after cooling, the film showed a multitude of cracks, probably as a result of the thermal and mechanical stress within the glass slide sandwich.

8. Luminescence Measurements

Steady-state photoluminescence (PL) experiments were carried out on a Photon Technology International (PTI) C720 spectrophotometer equipped with a Hamamatsu R928P photomultiplier. Excitation of molecular glasses was accomplished with a 2 mW non-polarized 543 nm green HeNe laser (Thorlabs HGR020, $1/e^2$ beam diameter 0.83 mm) equipped with a laser line filter (543.5 ± 2 nm, FWHM = 10 ± 2 nm). The angle of incidence with respect to the laser beam was 45°. Power densities were varied using reflective power density filters (Thorlabs) and measured with an optical power meter (Thorlabs PM100USB with photodiode power sensor S120VC). Liquid samples were measured in 10 mm path Suprasil® Hellma quartz cells using the spectrometer's Xe-lamp. Samples for phosphorescence measurements were deoxygenated by sparging with argon for 30 min.

9. PtOEP-Doped DPA-CH_2OH Molecular Glass Films

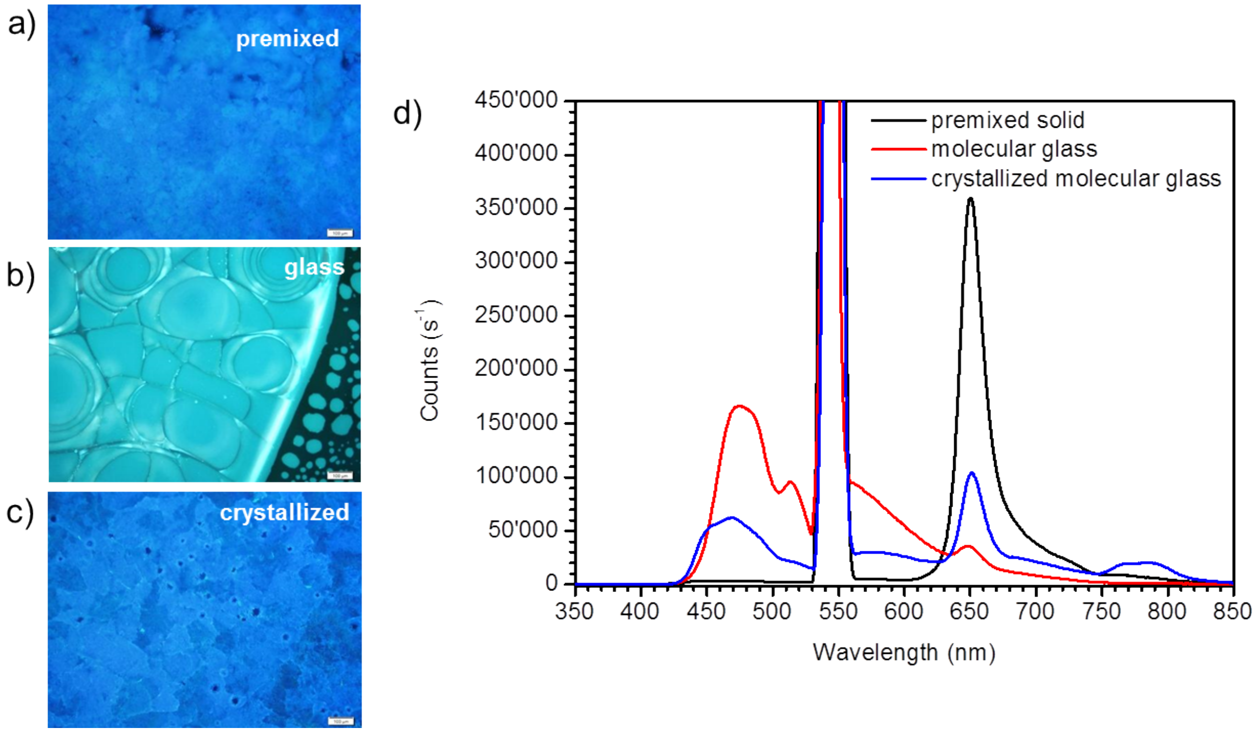

Fig. S12. a)-c) Fluorescence microscope images of DPA-CH_2OH doped with 0.025 mol% PtOEP (scale bars 100 µm): a) premixed solid, b) molecular glass (top left, film edge) and c) crystallized molecular glass (crystallized at 145°C for 165 min). d) Fluorescence emission spectra of samples a)-c) acquired upon irradiation with 2 mW 543 nm green HeNe laser.

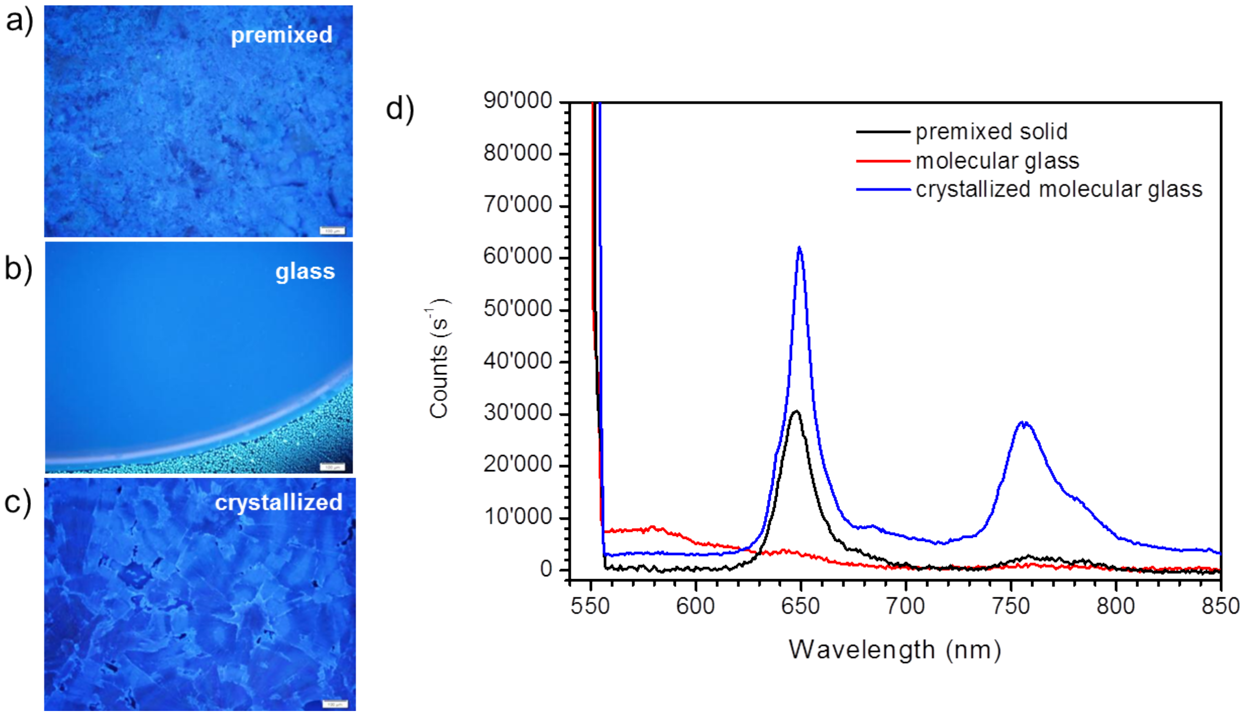

Fig. S13. a)-c) Fluorescence microscope images of DPA-CH_2OH doped with 0.7 mol% PtOEP (scale bars 100 µm): a) premixed solid, b) molecular glass (top left, film edge) and c) crystallized molecular glass (crystallized at 145°C for 165min). d) Laser red-shifted fluorescence emission spectra of samples a)-c) acquired upon irradiation with 2 mW 543 nm green HeNe laser.

10. PdOEP-Doped DPA-CH$_2$OH Molecular Glass Films

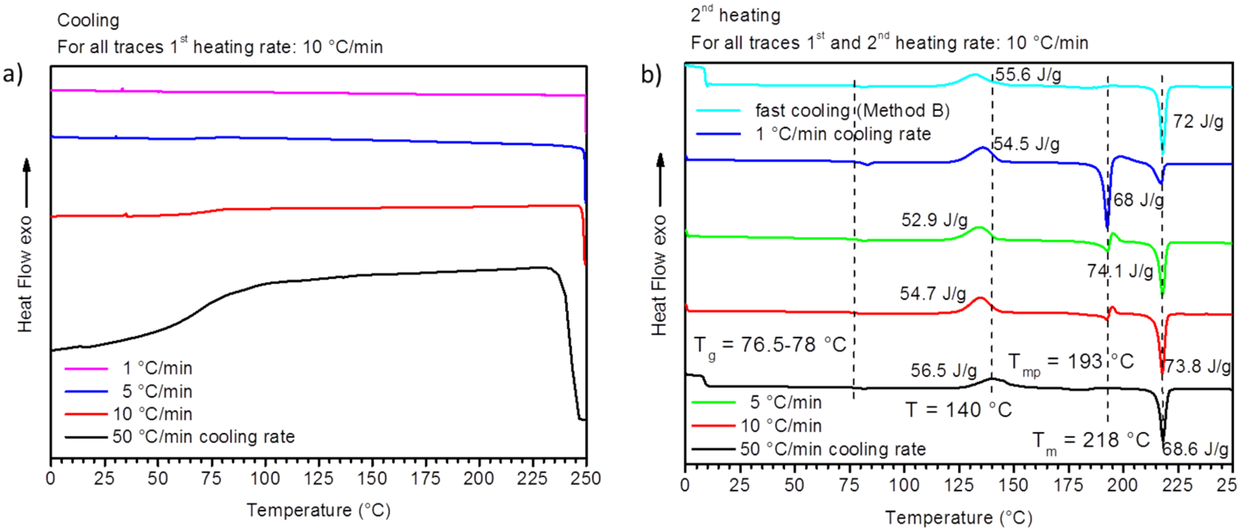

Fig. S14. a), b) DSC (cooling and second heating traces of samples cooled at different rates) of DPA-CH$_2$OH doped with 0.025 mol% PdOEP prepared according to Section 7. Heating and cooling rates, as well as the enthalpies of the various transitions are indicated in the graph.

No crystallization was observed during the cooling cycles and all the samples displayed the typical transitions for molecular glasses during the 2nd heating cycle (T_g, T_c, T_{m2}) except for an additional, minor polymorph melting at 193°C, arising when lower cooling rates were applied.

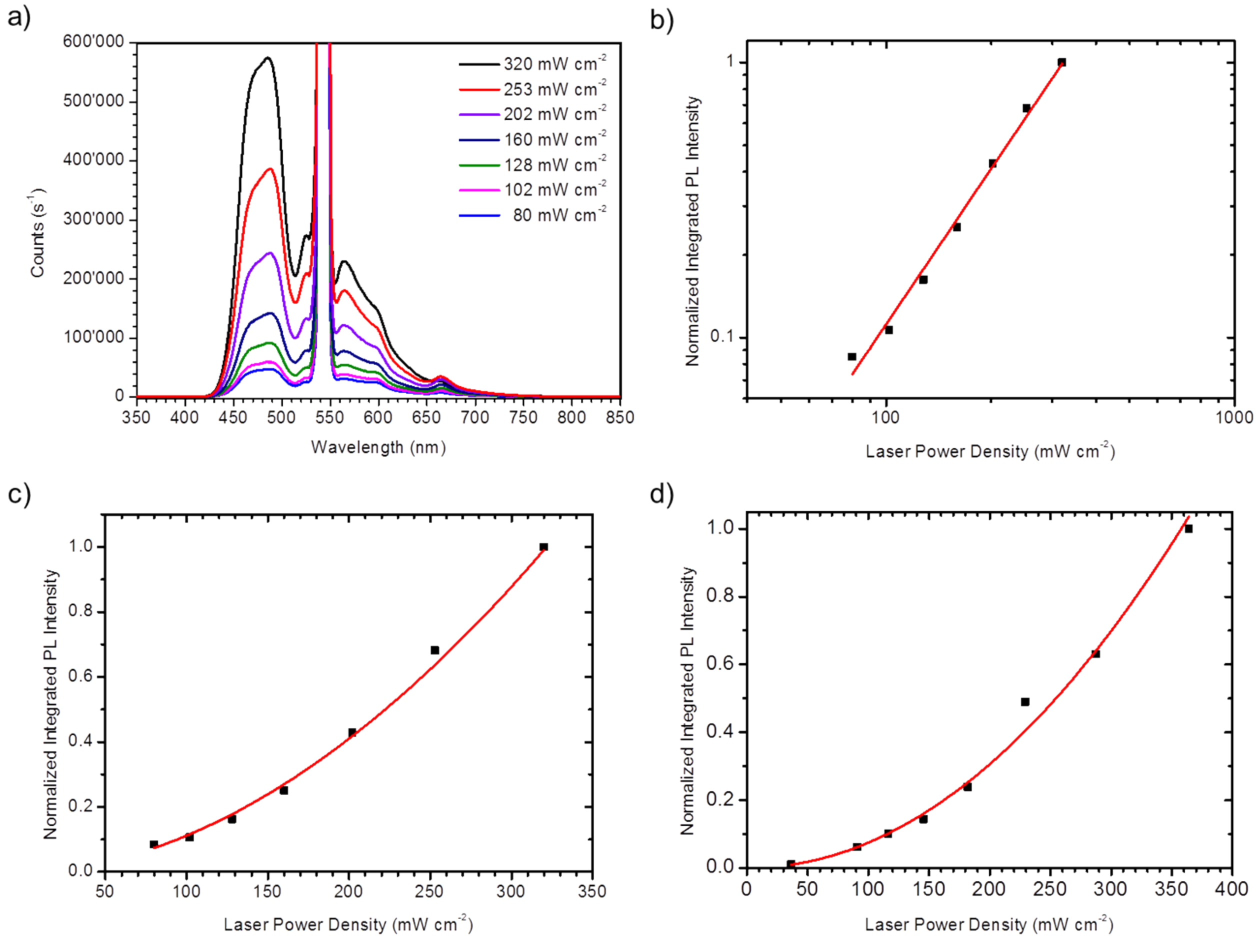

Fig. S15. a) Emission spectra of molecular glass films based on DPA-CH$_2$OH and PdOEP (0.025 mol%) upon irradiation with a 2 mW green HeNe laser (543 nm). The incident power density was varied, as indicated in the graph. b) Double logarithmic plot of the normalized integrated upconverted emission intensity (data from Fig. S15a, the maximum intensity was normalized to one) as a function of incident laser power (80-320 mW cm^{-2}). Linear regression of the data points showed a quadratic relationship with a slope of 1.88 +/- 0.08. c) Fig 3b and d) Fig S15b using double-linear representation.

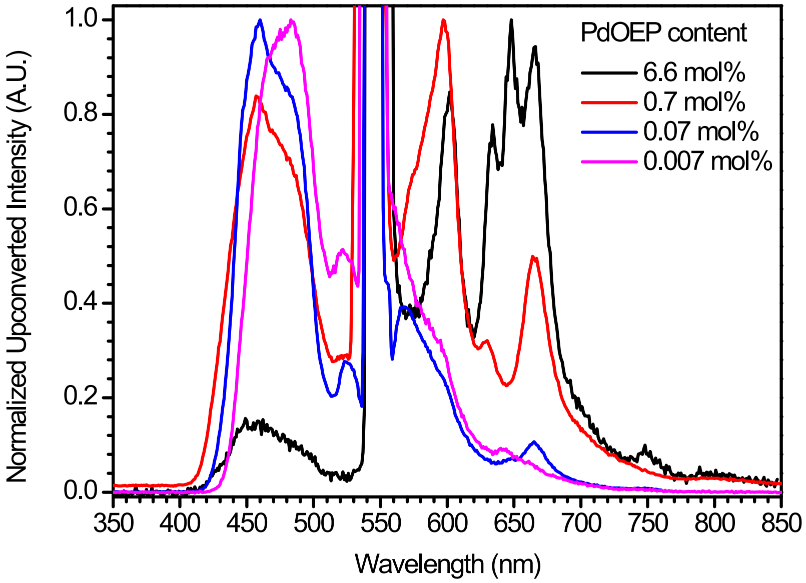

Fig. S16. Photoluminescence spectra of molecular glass films based on DPA-CH_2OH and PdOEP with PdOEP contents of 0.007 to 6.6 mol%, as indicated in the graph. All samples were irradiated with a 2 mW green HeNe laser (543 nm). Spectra were normalized to their respective maximum.

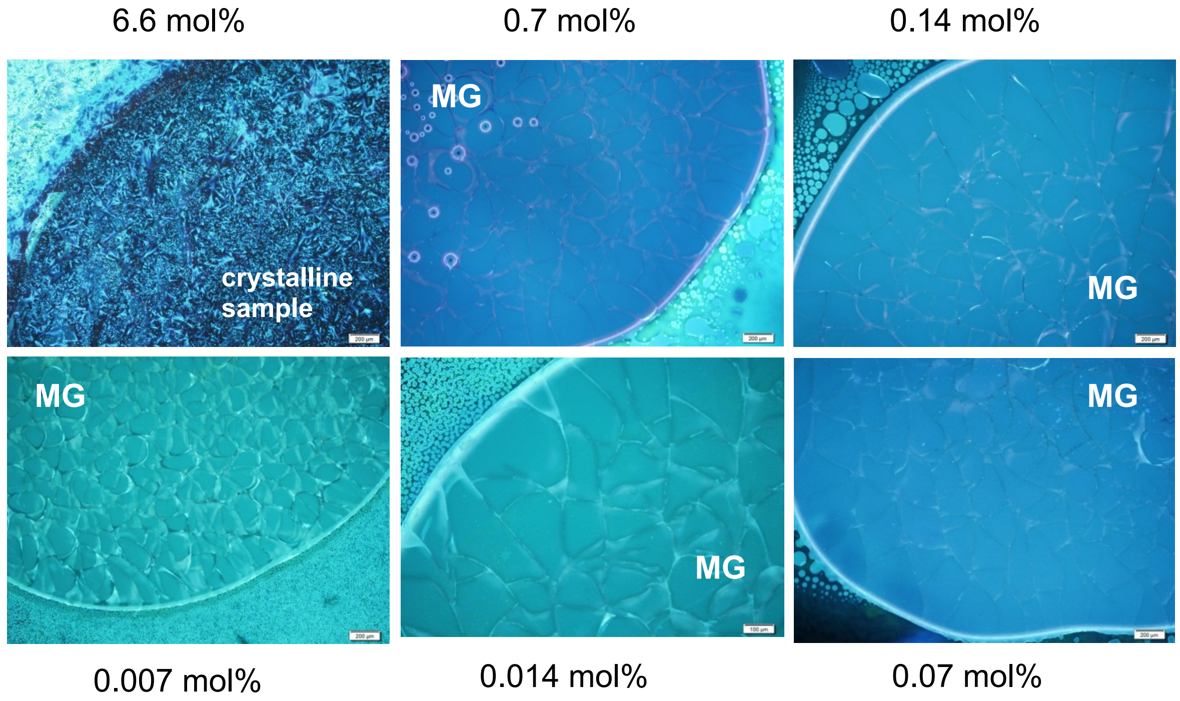

Fig. S17. Fluorescence microscope images of molecular glass films (film edge) based on DPA-CH_2OH and different PdOEP concentrations, as indicated in the figure. The scale bar corresponds to 200 µm.

At very high PdOEP-contents (6.6 mol%) no MG was obtained by cooling from the melt. MG with a higher content of PdOEP are darker.

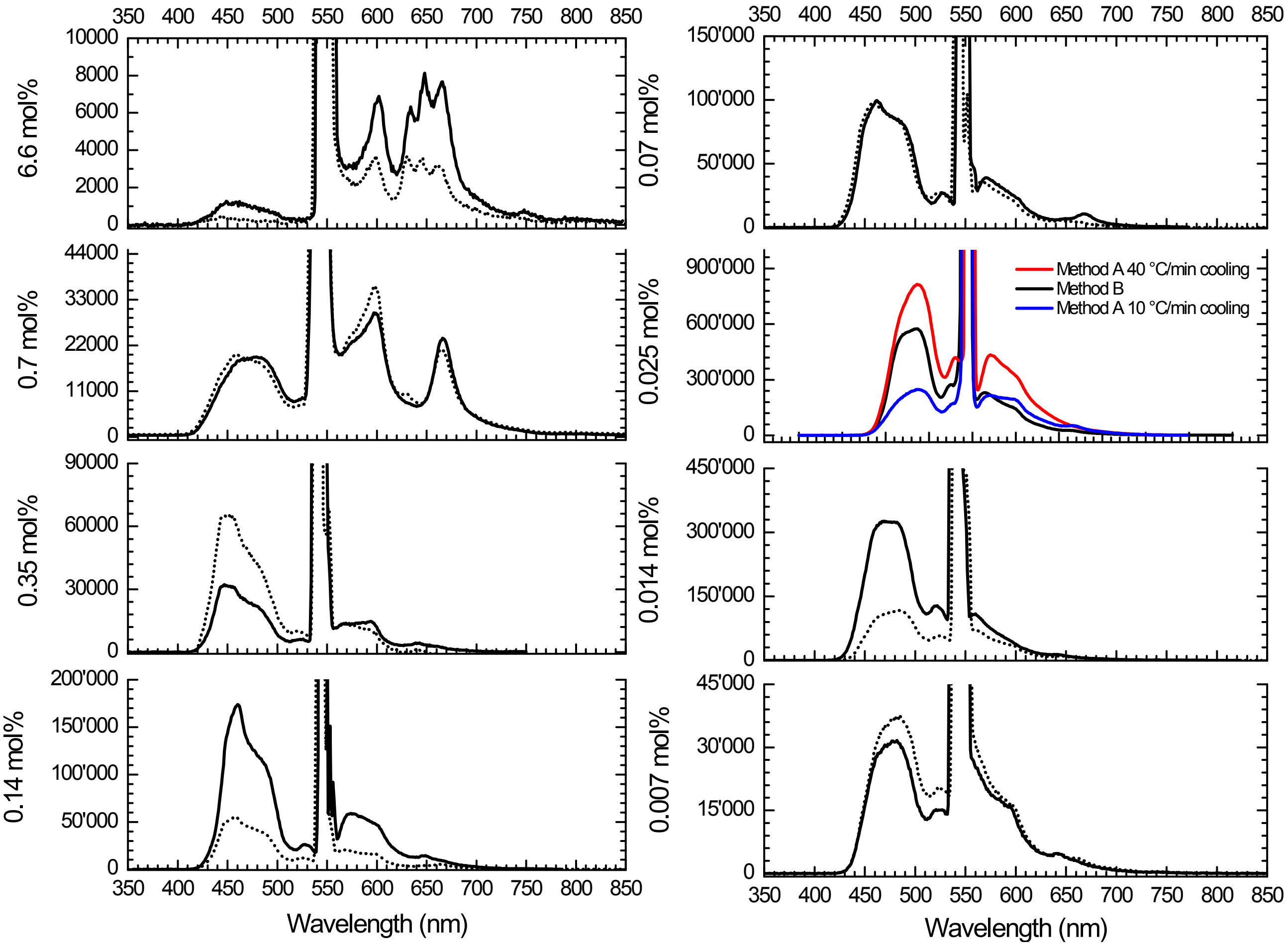

Fig. S18. Emission spectra of DPA-CH$_2$OH molecular glass films based on DPA-CH$_2$OH and PdOEP as a function of the PdOEP content, as indicated in the graphs. Spectra were acquired upon irradiation with a 2 mW green HeNe laser (543 nm). The solid and dotted curves represents two different molecular glasses of the same composition obtained by the method B. The graph at 0.025 mol% PdOEP content shows three samples; one produced by cooling by method B, the other two by method A cooling from 250 to 25°C at the defined rates of 10 and 40°C/min, respectively (see Section 7).

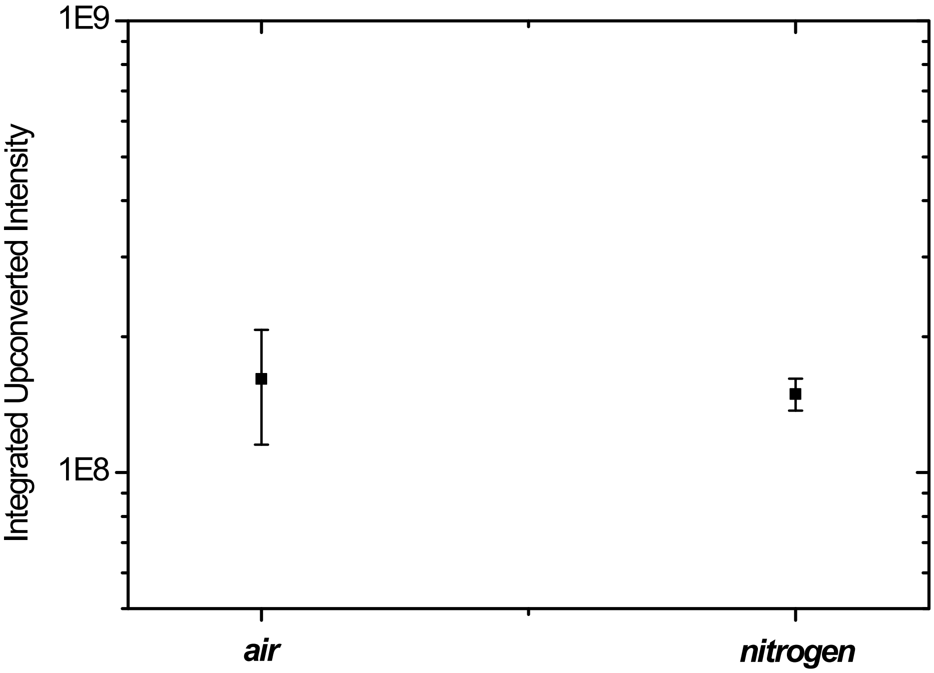

Fig. S19. Integrated upconverted intensity of a DPA-CH_2OH MG containing 0.025 mol% PdOEP measured under ambient conditions and nitrogen. Spectra at three different spots were acquired for each data point upon irradiation with a 2 mW green HeNe laser (543 nm, 300 mW cm^{-2}). No significant differences in integrated upconverted intensities were found.

11. Undoped DPA-CH$_2$OH Molecular Glasses

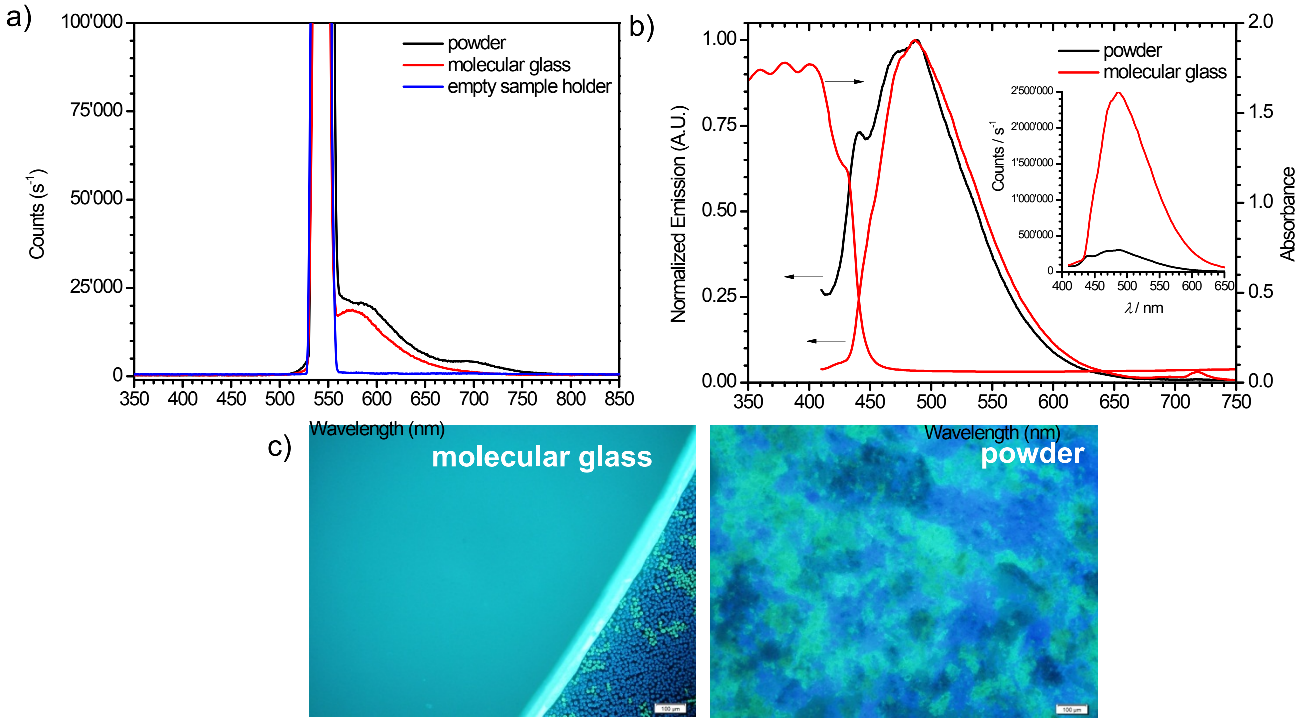

Fig. S20. a) Fluorescence emission spectrum of undoped DPA-CH$_2$OH powder, molecular glass and the empty sample holder upon irradiation with 2 mW green 543 nm HeNe laser. b) Normalized fluorescence emission spectra and absorption spectrum of undoped DPA-CH$_2$OH powder and molecular glass upon irradiation at 395 nm. Inset: Comparison of the absolute fluorescence intensities. c) Fluorescence microscope images of DPA-CH$_2$OH molecular glass and powder.

Irradiation of undoped DPA-CH$_2$OH powder and molecular glass with 2 mW @ 543 nm (Fig. S20a)) showed a weak emission band with maxima from 575-590 nm. No such band was observed with the empty sample holder only. The weak emission band at 575-590 nm may stem from raman scattering since the energetic difference ΔE (543 to 575-590 nm) = 1 to $1.5*10^3$ cm^{-1} lays in the range of vibrational energies of organic molecules.

Direct irradiation of DPA at 395 nm resulted in a higher fluorescence intensity for the molecular glass (inset Fig. S20b)) and in a slight red-shift of the normalized molecular glass emission (Fig. S20b), λ_{max}(powder) = 441 and 478 nm, λ_{max}(MG) = 487 nm). Higher fluorescence intensity of the molecular glass may be a consequence of reduced light scattering and/or a higher fluorescence quantum yield compared to the powder. For example, fluorescence quantum yields for DPA have been found dependent on its morphology (e.g. thin film, powder, single crystal). [2], [3]. The absence of the local emission maximum at 441 nm in the molecular glass may be a consequence from molecular disorder.

References

[1] X.M. Zhang, F. G. Bordwell, J. E. Bares, J.-P. Cheng, B.C. Petrie, *J. Org. Chem*. **1993**, *58*, 3051.

[2] Y. Fujiwara, R. Ozawa, D. Onuma, K. Suzuki, K. Yoza, K. Kobayashi, *J. Org. Chem.* **2013**, *78*, 2206.

[3] A. Azusa, S. Yamaguchi, *Chem. Commun*. **2009**, 3002.